

N-Benzoyl- and N-Sulfonyl-1,5-benzodiazepines: Comparison of Their Atropisomeric and Conformational Properties

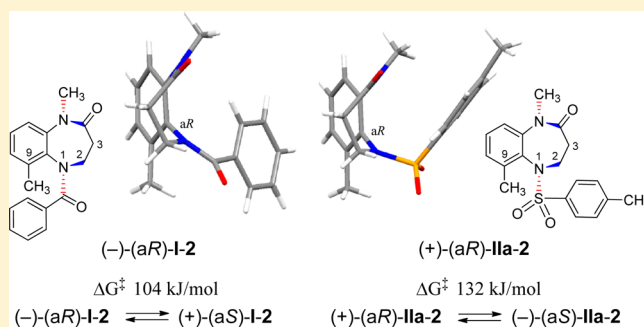
Tetsuya Yoneda,[†] Hidetsugu Tabata,[†] Jun Nakagomi,[†] Tomohiko Tasaka,[‡] Tetsuta Oshitari,[†] Hideyo Takahashi,[†] and Hideaki Natsugari^{*†}

[†]Faculty of Pharma Sciences, Teikyo University, 2-11-1 Kaga, Itabashi-ku, Tokyo 173-8605, Japan

[‡]Affinity Science Corporation, 4-1-1 Akasaka, Minato-ku, Tokyo 107-0052, Japan

S Supporting Information

ABSTRACT: The atropisomeric and conformational properties of 1,5-benzodiazepines with an *N*-sulfonyl (*p*-tosyl/mesyl) group (**IIa/b**) were investigated by comparison with those of the *N*-benzoyl congeners (**I**). Similar to **I**, when the Ar–N(SO₂) axis was frozen by a C9-substitution in the molecules, **IIa/b** were separated into the (aR)- and (aS)-atropisomers. The conformation of **IIa/b** revealed that the substituent (*p*-tolyl/methyl group) in the sulfonyl moiety occupies the position over the diazepine ring (folded form) in both the solid and solution states [e.g., (+)-(aR)-*N*-*p*-tosyl-1,5-benzodiazepin-2-one (**IIa-2**)], whereas that of **I** is *anti* to the diazepine ring [e.g., (–)-(aR)-*N*-benzoyl-1,5-benzodiazepin-2-one (**I-2**)], which was further supported by a computational study. The stereochemical stability also differed between the two congeners (e.g., ΔG^\ddagger : 104 kJ/mol for **I-2** and 132 kJ/mol for **IIa-2**).



INTRODUCTION

Nitrogen-containing benzo-fused seven-membered-ring heterocycles (e.g., 1,5-benzodiazepines) (Figure 1) occupy one of the

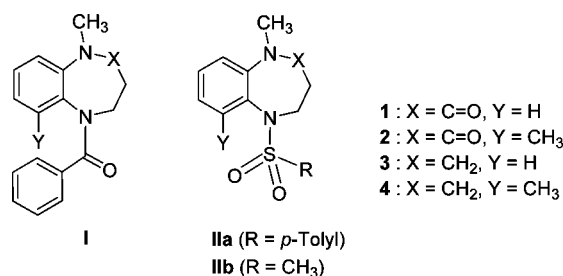


Figure 1. 1,5-Benzodiazepines (**1–4**) with an *N*-benzoyl group (**I**), *N*-*p*-tosyl group (**IIa**), and *N*-mesyl group (**IIb**).

most exalted places among molecules with beneficial biological activity.¹ The conformation of these heterocycles has been extensively investigated to gain insight into the structures of these relatively flexible rings. The important point is that a conformational change in the seven-membered-ring sometimes causes chirality due to the axis or plane in relation to the planar benzo group of the bicyclic molecule, which targets molecules such as receptors and enzymes to exert biological activity.² Thus, far, we have investigated the conformation of several benzo-fused seven-membered-ring nitrogen-heterocycles to reveal the atropisomeric properties in relation to the biological activity.³ In our previous communication,^{3f} atropisomerism in

N-benzoyl-1,5-benzodiazepines (for **I-1**, **I-2**, and **I-4**) was described in which the *cis/trans*-amide rotamers around the N–C(=O) bond and (aS)/(aR)-axial isomers⁴ based on the Ar–N(CO) (sp²–sp²) axis were considered (Figure 2). Although the conformational change in the molecules without a substituent at the *ortho*-position (C9) on the benzene ring (Y = H) was too rapid for isolation of the isomers at room temperature, the molecules with a substituent (Y = CH₃) at C9 were conformationally “frozen” and could be separated into the (aS)- and (aR)-axial isomers using chiral HPLC. That study led to the finding of the importance of axial chirality in exerting the biological activity of the vaptan class of arginine–vasopressin receptor ligands (e.g., mozavaptan⁵ and tolvaptan⁶); although a pair of atropisomers of mozavaptan itself is rapidly interconverting and inseparable, the receptors in the body recognize only one conformational isomer with (*cis*, aS, *5S*)-stereochemistry (Figure 3).

In addition to the *N*-benzoyl derivatives of 1,5-benzodiazepines (**I**), we investigated the congener *N*-sulfonyl (*p*-tosyl/mesyl) derivatives (**IIa/b**) (Figure 1). Although the sulfonamide group is the important functional moiety used in various biologically active compounds,⁷ its chemical nature is not as well understood as that of the amide group. Furthermore, there have been few studies on the atropisomerism caused by the Ar–N(SO₂) axis. Recent publications from the Merck group on the *N*-sulfonyl derivatives of pyrido- and benzo-fused tricyclic

Received: April 15, 2014

Published: May 16, 2014

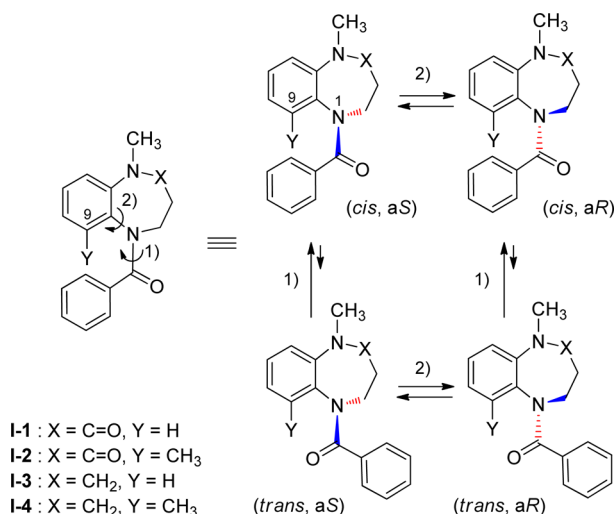


Figure 2. Conformation of *N*-benzoyl-1,5-benzodiazepines (I-1–I-4): (1) rotation around the N–C(=O) bond to form *cis*- and *trans*-rotamers and (2) rotation around the Ar–N axis to form (a*S*)- and (a*R*)-atropisomers.

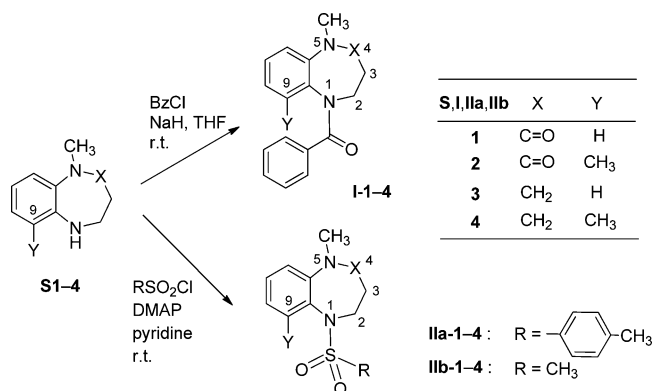
diazepine (MK-7725) (Figure 3) as a bombesin receptor subtype 3 agonist,⁸ in which atropisomerism was first disclosed as an interesting unusual chirality,⁹ prompted us to report our study on the atropisomeric properties of *N*-sulfonyl derivatives of 1,5-benzodiazepines (IIa/b) in detail by comparing them with those of the *N*-benzoyl congeners (I).

RESULTS AND DISCUSSION

Preparation of *N*-Benzoyl- and *N*-Sulfonyl-1,5-benzodiazepines. The 1,5-benzodiazepine derivatives with an *N*-benzoyl group, I (1–4), *N*-*p*-toluenesulfonyl (tosyl) group, IIa (1–4), and *N*-methanesulfonyl (mesyl) group, IIb (1–4), were prepared from the corresponding amines of the heterocycles (S1–4) by conventional methods using benzoyl chloride, tosyl chloride, and mesyl chloride, respectively (Scheme 1).¹⁰ Compounds with a methyl group at C9 on the benzene ring (Y = CH₃) (I-2/4, IIa-2/4, and IIb-2/4) were prepared to provide a rotational barrier for the axis and to freeze the conformation of the molecules.

Conformation of the *N*-Benzoyl-1,5-benzodiazepines (I). The stereochemistry of the *N*-benzoyl-1,5-benzodiazepin-4-ones (I-1/2)^{3f} and *N*-benzoyl-1,5-benzodiazepines (I-3/4)^{3f} was first investigated. As shown in Figure 2, four stereoisomers [i.e., the *cis/trans*-amide rotamers around the N–C(=O) bond and (a*S*)/(a*R*)-axial isomers based on the Ar–N(CO) axis] were assumed to exist, and their presence was confirmed by isolating the (a*S*)- and (a*R*)-axial isomers of I-2 and I-4 with a

Scheme 1. Preparation of 1,5-Benzodiazepines with an *N*-Benzoyl Group (I-1–4), *N*-*p*-Tosyl Group (IIa-1–4), and *N*-Mesyl Group (IIb-1–4)



methyl group at C9 on the benzene ring (Y = CH₃). Compound I-2 was shown to exist as an equilibrium mixture of *cis/trans*-amide rotamers in solution (CDCl₃) with the *cis/trans* ratio of 10:1 by ¹H NMR,¹¹ while I-1, I-3, and I-4 only showed signals of the *cis*-isomer at room temperature. The physicochemical properties of I (1–4) are shown in Table 1. Fortunately, the absolute structures of (–)-(a*S*,a*R*)-I-2, (+)-(a*S*,a*S*)-I-2, and (+)-(a*S*,a*S*)-I-4 could be determined by X-ray structure analysis (Figure 4, Table 2).¹² The crystal structures of (+)-(a*S*,a*S*)-I-2 and (+)-(a*S*,a*S*)-I-4 are similar, with the two benzene rings in a proximal location, but differ in the orientation of the C3 methylene moiety (i.e., the seven-membered ring with a boatlike and chairlike conformation, respectively) (Figure 4). The difference may be explained as follows: Because I-2 (X = C=O) has a lactam moiety, two Ar–N(CO) axes (a¹ and a²) exist in the molecule to take a conformation with the relative stereochemistry of (a¹R*, a²R*),^{3d,f,13} which inevitably constrains the seven-membered ring to take a boatlike form, whereas in the fully reduced diazepine ring of I-4 (X = CH₂) the conformation is more flexible and takes an unconstrained form (i.e., a chairlike form in this case). The conformation of the diazepine-ring in solution was inspected by the coupling pattern of the methylene protons in the ¹H NMR spectrum. The observed values of the vicinal coupling (³*J*) in the lactam I-2 corresponded well with those estimated from the torsion angles obtained from the X-ray crystal structure (a boatlike form) by the Karplus equation.¹⁴ Those in the reduced diazepine I-4, on the other hand, did not correspond with the ³*J*_{H,H} values estimated from the crystal structure (a chairlike form), and no large ³*J*_{H,H} values (>9 Hz) were observed. These data imply that the reduced diazepine-ring of I-4 is flexible to

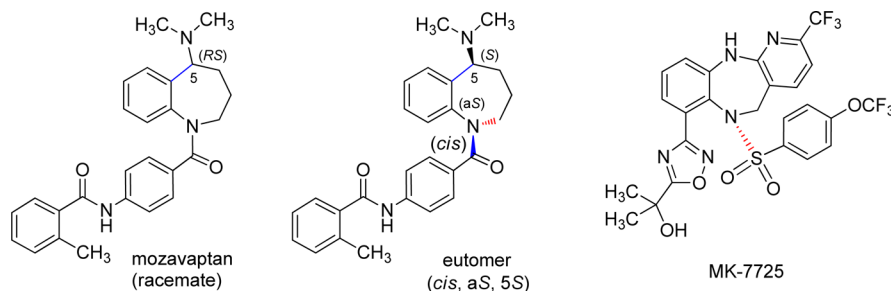
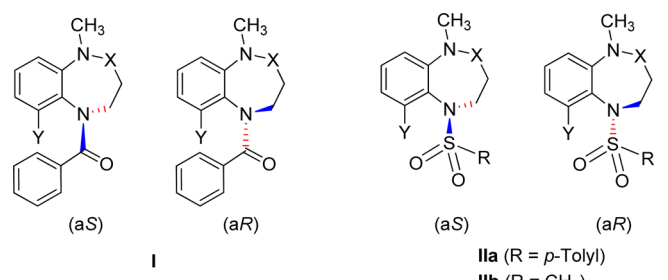


Figure 3. Mozavaptan, the plausible eutomer of mozavaptan, and MK-7725.

Table 1. Physicochemical Properties of the Atropisomers of *N*-Benzoyl-, *N*-*p*-Tosyl-, and *N*-Mesyl-1,5-benzodiazepines (I, IIa, and IIb)


I, IIa, IIb	X	Y	I (benzoyl)			IIa (<i>p</i> -tosyl)			IIb (mesyl)			
			$[\alpha]_D^{23}$ ^a	ΔG^\ddagger (kJ/mol)	racemization ^b	$[\alpha]_D^{23}$ ^a	ΔG^\ddagger (kJ/mol)	racemization ^b	$[\alpha]_D^{23}$ ^a	ΔG^\ddagger (kJ/mol)	racemization ^b	
1	C=O	H	<i>c</i>	67		<i>c</i>	59		<i>c</i>	54		
2	C=O	CH ₃	(aS)	+113.1	104	50 °C, 5 h ^d	-155.2	132	150 °C, 2 h ^{e,f}	-159.1	132	150 °C, 2 h ^{e,f}
			(aR)	-115.0			+159.7			+164.1		
3	CH ₂	H	<i>c</i>	68		<i>c</i>	48		<i>c</i>	48		
4	CH ₂	CH ₃	(aS)	+151.0	96	37 °C, 2 h	-134.0	105	50 °C, 7 h ^g	-88.5	105	50 °C, 7 h ^g
			(aR)	-146.7			+136.6			+81.4		

^aIn CH₃OH and for each concentration (*c*); see the Experimental Section. ^bConditions required for racemization in toluene. ^cNot separable at room temperature. ^dIsomerized to 50% ee at 37 °C after 6 h in toluene. ^eIn DMF. ^fNot isomerized at 80 °C after 4 h in toluene. ^gIsomerized to 50% ee at 37 °C after 8 h in toluene.

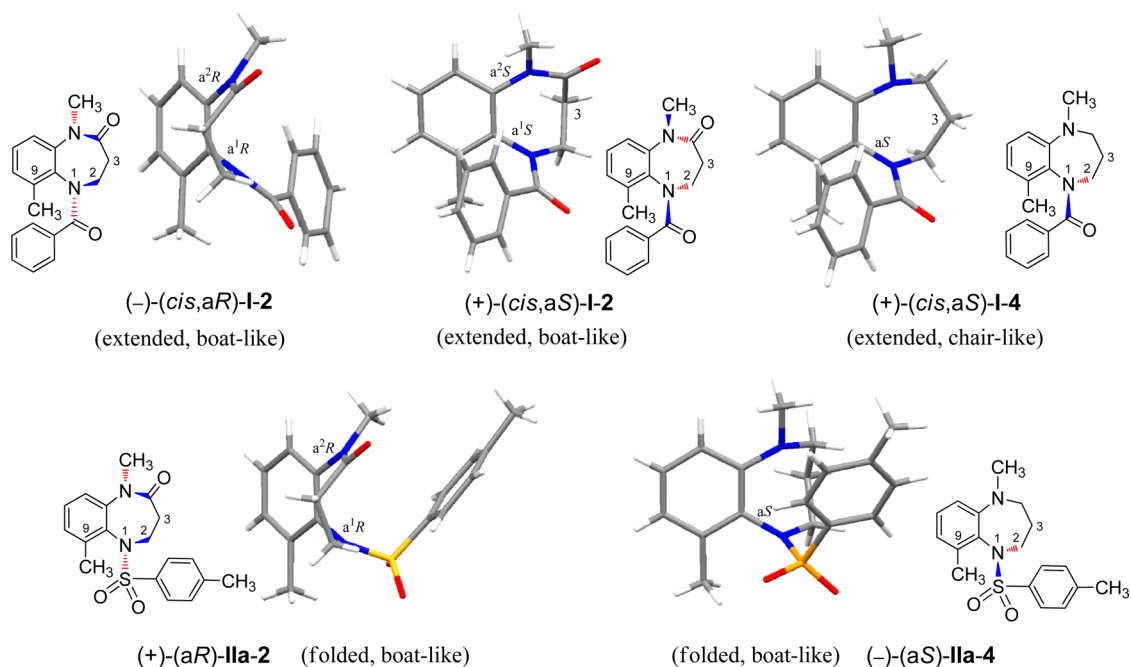


Figure 4. X-ray crystal structures of (aR)-I-2, (aS)-I-2, (aS)-I-4, (aR)-IIa-2, and (aS)-IIa-4.

take various conformations in solution at room temperature (i.e., the methylene signals observed in the ¹H NMR spectrum are the average ones of the chair- and boatlike conformers), which seemed to be a common aspect of the reduced diazepine ring system in solution, e.g., that of IIa-4 and IIb-4 described below (cf. a drawing of IIb-4 in Figure 7).

Conformation of the *N*-Sulfonyl-1,5-benzodiazepines (IIa and IIb). The stereochemistry of the *N*-sulfonyl derivatives [IIa (1–4) (tosyl) and IIb (1–4) (mesyl)] was next investigated by comparing it with that of the corresponding *N*-benzoyl derivatives I (1–4). The results are summarized in Tables 1 and 2. First, *N*-tosyl-1,5-benzodiazepin-4-ones (X =

C=O) [IIa-1 (Y = H)/IIa-2 (Y = CH₃)] were examined in detail. We originally expected that the sulfonamides IIa-1/2 would also exhibit atropisomeric properties similar to I-1/2, although the nature of the sulfonamide is not as well understood as that of the amide. The results conformed to our expectations, i.e., although the (aS)/(aR)-atropisomers of IIa-1 were inseparable, those of IIa-2 were sufficiently stable to be separated and isolated with chiral HPLC at room temperature. However, the conformations of IIa-1/2 were unexpectedly shown to be significantly different from those of I-1/2. First, the separated (+)-enantiomer of IIa-2 ($[\alpha]_D^{23} +159.7$) was subjected to X-ray structural analysis to reveal

Table 2. Conformation (X-ray and ^1H NMR Analyses) of *N*-Benzoyl-, *N*-*p*-Tosyl-, and *N*-Mesyl-1,5-benzodiazepines (I, IIa, and IIb)

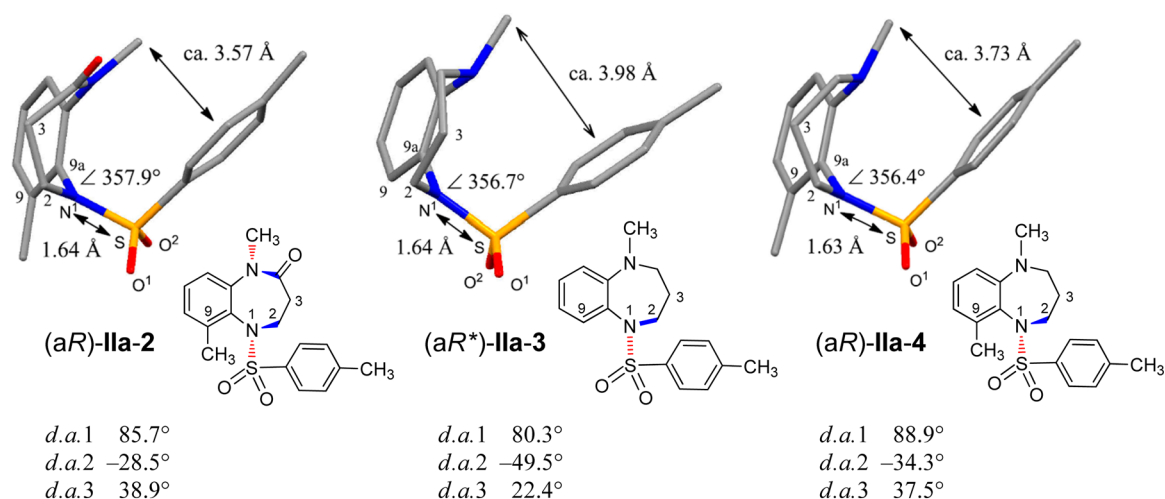
		X-ray crystal analysis			^1H NMR	
		conformation		dihedral angle $\angle\text{C}^9\text{-C}^{9a}\text{-N}^1\text{-S}$ (or C) (deg)	N^3CH_3	
	extended/ folded ^a	boat/ chair ^b			δ (ppm)	$\Delta\delta$ (vs S) ^c
<i>N</i> -benzoyl (I)						
I-1	N.A. ^d				3.50	0.15
I-2	(+)-(aS)	extended	boat	-61.82	3.51	0.18
I-2	(-)-(aR)	extended	boat	+61.73		
I-3	N.A. ^d				2.96	0.03
I-4	(+)-(aS)	extended	chair	-69.57	2.94	0.03
<i>N</i> -tosyl (IIa)						
IIa-1	N.A. ^d				2.59	-0.76
IIa-2	(+)-aR	folded	boat	+85.68	2.58	-0.75
IIa-3	racemate	folded	chair	± 80.29	2.36	-0.57
IIa-4	(-)-aS	folded	boat	-88.49	2.23	-0.70
IIa-4	(+)-aR	folded	boat	+88.85		
<i>N</i> -mesyl (IIb)						
IIb-1	racemate	folded	boat	± 75.94	3.35	0
IIb-2	(-)-aS	extended	boat	-93.09	3.35	0.02
IIb-2	racemate	folded	boat	± 84.35		
IIb-3	racemate	folded	chair	± 83.61	2.85	-0.08
IIb-4	(-)-aS	folded	boat	-88.36	2.82	-0.09
IIb-4	(+)-aR	folded	boat	+89.20		

^aOrientation of the substituent in the *N*-benzoyl- or *N*-sulfonyl moiety relative to the 1,5-benzodiazepine ring. ^bConformation of the 1,5-benzodiazepine ring. ^cDifference of the chemical shift compared to that of the corresponding starting materials (S1–4). For reference, the chemical shifts of N^3CH_3 (δ , ppm) of S1, S2, S3, and S4, are 3.35, 3.33, 2.93, and 2.91, respectively. ^dN.A.: not analyzed.

that the 1,5-benzodiazepine ring exists in a boatlike form with (aR)-stereochemistry¹² (Figure 4, Table 1). Interestingly, the (+)/(-)-angle of optical rotation α of (aR)-IIa-2 is reversed

compared with that of the *N*-benzoyl derivative (aR)-I-2 ($[\alpha]_{\text{D}} -115.0$). As shown in Figure 4, the benzene ring of the tosyl moiety of IIa-2 is differently oriented from that of the benzoyl moiety of (aR)-I-2, i.e., the benzene ring of IIa-2 locates over the diazepine ring (folded form), whereas that of I-2 locates *anti* to the diazepine ring (extended form) (Figure 4). Also noteworthy is the position of the oxygen atoms of the sulfonyl (SO_2) moiety in IIa-2, which locate so as to interweave with the N-SO_2 axis [dihedral angles $\angle\text{O}^2\text{-S-N}^1\text{-C}^{9a}$ (*d.a.* 2) and $\angle\text{O}^1\text{-S-N}^1\text{-C}^2$ (*d.a.* 3) in Figure 5 were -28.5° and 38.9° , respectively], whereas the oxygen of the carbonyl (C=O) moiety in I-2 is on the amide ($>\text{N-C=O}$) plane. In the crystal structure of IIa-2, since the sum of angles around the nitrogen atom in the $>\text{N-SO}_2$ moiety is 357.9° , the nitrogen atom possesses an sp^2 -like nature and the bond length between N-S (1.64 Å) also suggests the double bond character of the S-N bond.¹⁵ These data imply that the $>\text{N-S}$ moiety forms a plane, and furthermore, the dihedral angle $\angle\text{C}^9\text{-C}^{9a}\text{-N}^1\text{-S}$ (*d.a.* 1 in Figure 5) of 85.7° indicates that the two planes (benzene and $>\text{N-S}$ moiety) are approximately orthogonally oriented to form the axial chirality (Figure 5). The dihedral angle of IIa-2 (85.7°) indicates that the sulfonyl moiety is more distorted than that of the benzoyl derivatives (I-2: 61.7°) (Table 2). The ^1H NMR (CDCl_3) spectrum of IIa-2 showed that the folded form observed in the crystal state exists in solution as well, i.e., the chemical shift of the NCH_3 signals of IIa-2 is observed at a higher field (2.58 ppm) compared with that of I-2 (3.51 ppm). The markedly higher shift in IIa-2 can be explained as due to the NCH_3 group locating over the benzene ring of the tosyl moiety.

Similar structural aspects were observed in the *N*-tosyl derivative of the reduced 1,5-benzodiazepines ($\text{X} = \text{CH}_2$) [IIa-3 ($\text{Y} = \text{H}$) and IIa-4 ($\text{Y} = \text{CH}_3$)]. The compounds IIa-3 (racemate) and IIa-4 [both (-)-aS and (+)-aR atropisomers] were subjected to X-ray structural analysis (Figures 4 and 5), which revealed that the 1,5-benzodiazepine ring in IIa-3 exists as a chairlike form and that in IIa-4 as a boatlike form and that the benzene ring of the tosyl moiety in IIa-3/4 locates over the



$$d.a.1 = \angle\text{C}^9\text{-C}^{9a}\text{-N}^1\text{-S}, \quad d.a.2 = \angle\text{O}^2\text{-S-N}^1\text{-C}^{9a}, \quad d.a.3 = \angle\text{O}^1\text{-S-N}^1\text{-C}^2$$

Figure 5. Dihedral angles (*d.a.*1–3), sum of the angles around nitrogen N^1 , and distances between $\text{N}^1\text{-S}$ and $\text{NCH}_3\text{-Ar}$ in the *N*-tosyl derivatives (aR)-IIa-2, (aR*)-IIa-3, and (aR)-IIa-4, obtained from the CIF data of X-ray crystal analysis. The structure of (aR*)-IIa-3 is extracted from the CIF data of the racemate.

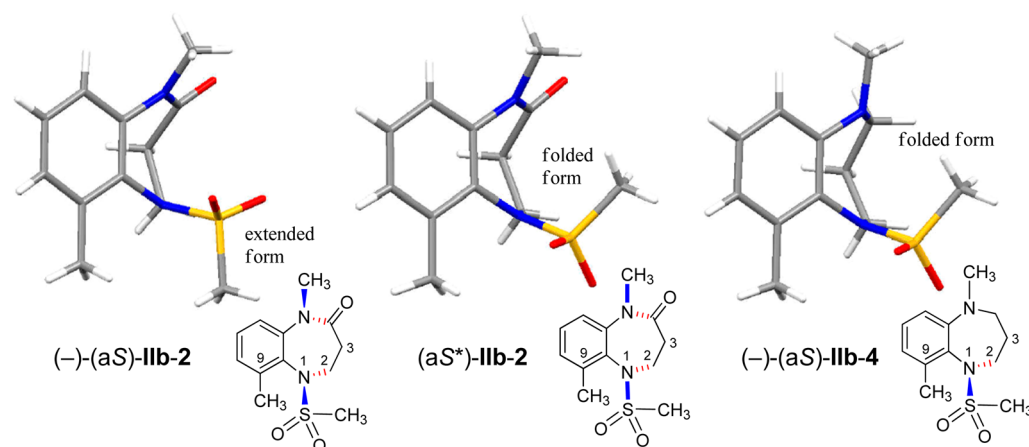


Figure 6. X-ray crystal structures of the *N*-mesyl derivatives $(-)-(aS)$ -**IIb-2**, (aS^*) -**IIb-2**, and $(-)-(aS)$ -**IIb-4**. The structure of (aS^*) -**IIb-2** is extracted from the CIF data of the racemate **IIb-2**.

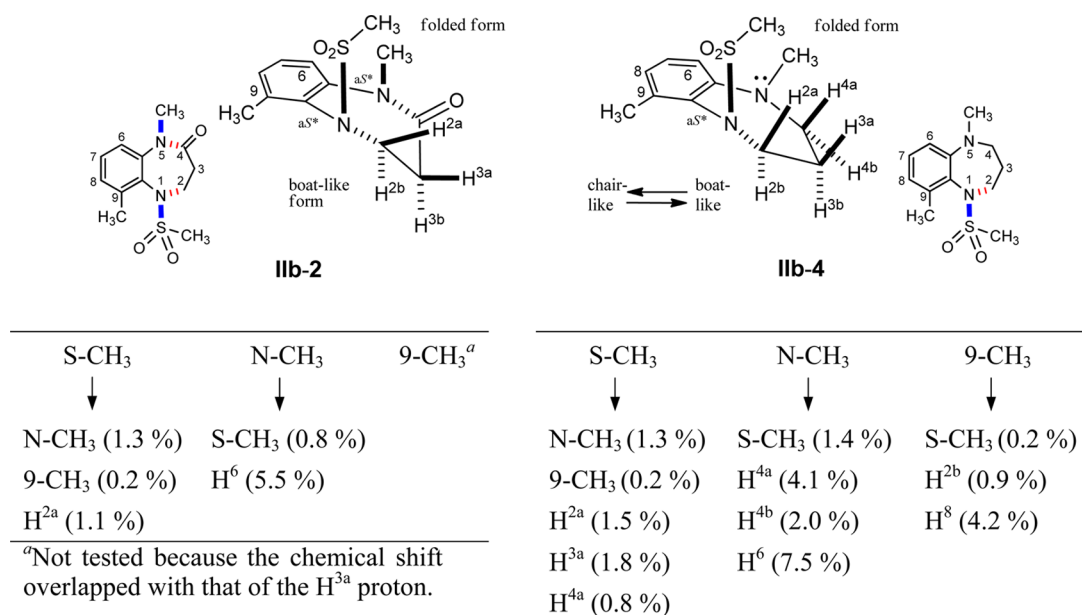


Figure 7. NOEDS experiment on **IIb-2** and **IIb-4** after irradiation at the CH₃ protons: % enhancement after irradiation at the CH₃ protons is shown in parentheses.

diazepine ring (folded form), as was observed in **IIa-2**. The dihedral angle (*d.a.1* in Figure 5) of **IIa-3** (80.3°) and **IIa-4** (*aS*, 88.5°/*aR*, 88.9°) reveals an important aspect of the conformation of **IIa-3/4**; i.e., the C9-methyl group in **IIa-4** pushes the tosyl group toward the diazepine ring to force the C3 methylene to adopt a rigid boatlike form of the ring, whereas **IIa-3** without such an effect possesses a ring with a chairlike form. The chemical shift of the NCH₃ signal in the ¹H NMR spectrum of **IIa-3/4** was also observed at a higher field (2.36 and 2.47 ppm, respectively) compared with that of **I-3** and **I-4** (2.96 and 2.94 ppm, respectively) (Table 2), indicating again that **IIa-3/4** take the folded conformation in both the solid and solution states. As for the diazepine-ring conformation of **IIa-3/4** in solution, a similar flexible aspect as that of **I-4** (as mentioned above) was shown by ¹H NMR analysis (the ³J_{H,H} values of the methylene protons) of **IIa-4**. The properties of the *N*-mesyl derivatives of 1,5-benzodiazepines **IIb** (1–4) were similar to those of the tosyl derivatives **IIa** (1–4) (Tables 1 and 2 and Figure 6). The only exception is the crystal structure of $(-)-(aS)$ -**IIb-2**, which exhibited an extended

form and a large dihedral angle (−93.1°) (Figure 6). Since the X-ray crystal structure of the racemate of **IIb-2** had a folded form similar to that of the corresponding tosyl derivative (**IIa-2**), the unique property of $(-)-(aS)$ -**IIb-2** is assumed to be caused by crystallization, although we do not yet have sufficient information to support this assumption. In solution, on the other hand, **IIb-2** was deduced to take the folded form based on the results of the nuclear Overhauser enhanced differential spectroscopy (NOEDS) and NOESY experiments; i.e., NOE enhancement and correlation were observed between the two CH₃ protons in the SO₂–CH₃ and N–CH₃ groups (Figure 7).¹⁶ Similar NOE correlations were also observed for **IIb-4**, indicating that **IIb-4** takes the folded form (Figure 7).

Computational Study on the Stable Conformation of *N*-Benzoyl- and *N*-Tosyl-1,5-benzodiazepines (for **I-4 and **IIa-4**).**¹⁷ The stable conformation of *N*-benzoyl- and *N*-tosyl-1,5-benzodiazepines was estimated in a computational study using *(aS)*-**I-4** and *(aS)*-**IIa-4**. First, we calculated the energy surfaces defined by two dihedral angles to obtain stable conformers for these compounds (Figure 8) at the RHF/STO-

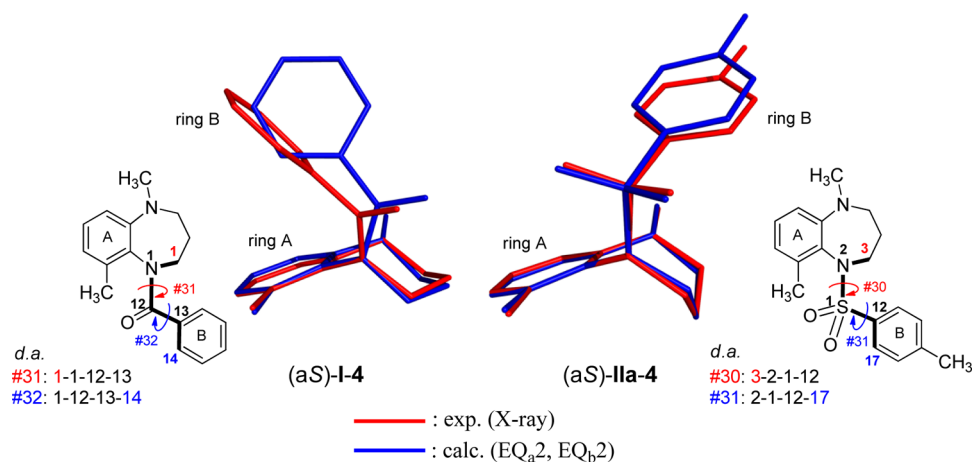


Figure 8. Overlap between the stable conformers of (aS)-I-4/(aS)-IIa-4 obtained by the X-ray crystal analysis (red line) and computational study using RB3LYP/6-31G(d) (blue line) and definition of dihedral angles (d.a.) of (aS)-I-4 and (aS)-IIa-4 for exploring the energy surface.

3G level. For the stable conformers extracted from the energy surfaces, the geometries were further optimized at a more accurate level, i.e., RB3LYP/6-31G(d). The most stable conformations for I-4 and IIa-4 obtained in these calculations are shown in Figure 8 (blue lines), which are consistent with those obtained experimentally from X-ray crystallography and ¹H NMR analysis (Figure 8, red lines).

Stereochemical Stability of *N*-Benzoyl- and *N*-Sulfonyl-1,5-benzodiazepines (I, IIa, and IIb). The stereochemical (thermodynamic) stability of I, IIa, and IIb was next examined (Figure 9, Table 1). First, the stability of the compounds

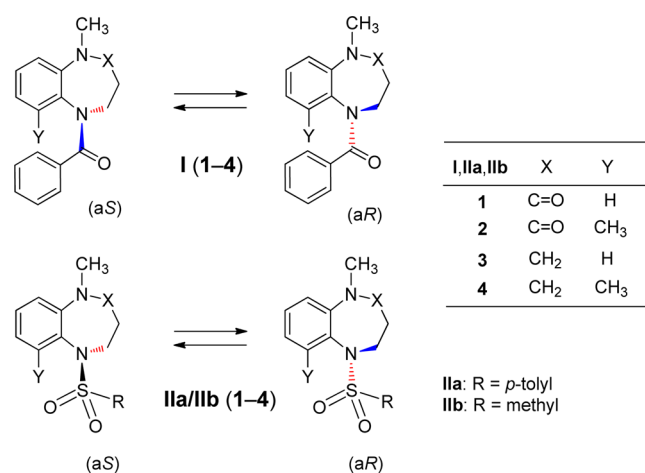


Figure 9. Stereochemical (thermodynamic) stability of the atropisomers of I, IIa, and IIb.

without a substituent at the C9 position (Y = H) (1, 3) (I, IIa, and IIb), of which the conformational change is too rapid to isolate the isomers at room temperature, was investigated. In the ¹H NMR spectra, each of the methylene protons of the diazepine ring of these compounds was observed as a separated peak (i.e., as diastereotopic protons), which were observed as relatively sharp ones in the benzoyl derivatives (I-1/3) and as broad signals in the sulfonyl derivatives (IIa-1/3 and IIb-1/3), suggesting that the conformational change at the Ar–N(CO) axis accompanied by the flipping of the diazepine ring is slower in the benzoyl derivatives than in the sulfonyl ones on the NMR time scale at room temperature (23 °C, 296 K). The

activation free-energy barrier to rotation (ΔG^\ddagger) estimated by the variable temperature ¹H NMR (VT NMR)¹⁸ for I-1/3, IIa-1/3, and IIb-1/3 (Table 1) supported this assumption. In the VT NMR spectrum of I-1 (Figure 10, left), the signals of the diastereotopic (and resolved) methylene protons of the diazepine ring coalesced at around 363 K (for H^{2a/2b}) and 333 K (for H^{3a/3b}) with the ΔG^\ddagger value of 67 kJ/mol, and sharpened at lower temperatures (below 296 K) as expected. In addition, compound I-3 showed a similar VT NMR pattern with a ΔG^\ddagger value of 68 kJ/mol. On the other hand, the sulfonyl derivatives (IIa-1/3 and IIb-1/3) showed lower ΔG^\ddagger values compared with the benzoyl ones (Table 1): the ΔG^\ddagger values estimated for IIa-1, IIa-3, IIb-1, and IIb-3 were 59, 48, 54, and 48 kJ/mol, respectively. It is interesting to note that the N–CH₃ signal of IIa-1 downshifted slightly when the temperature was elevated (e.g., δ 2.49 ppm at 243 K and 2.64 ppm at 323 K (Figure 10, right), indicating that the benzene ring of the tosyl group located over the N–CH₃ group sways slightly at elevated temperatures.

The stereochemical stability of 2 and 4 (Y = CH₃) (I, IIa, and IIb) was next examined using the separated atropisomers. The ΔG^\ddagger values were estimated experimentally from the conversion profiles between the enantiomers.¹⁹ The ΔG^\ddagger values and conditions required for racemization of the enantiomers are shown in Table 1. The diazepines with the lactam moiety (X = C=O) (I-2, IIa-2, and IIb-2) have higher energy barriers than the corresponding fully reduced diazepines (X = CH₂) (I-4, IIa-4, and IIb-4) (Table 1), which reflects the conformational rigidity of the diazepine rings; i.e., since the lactam derivatives possess two axes, the conformation is assumed to be more rigid than that of the fully reduced diazepines.

It is noteworthy that, among the compounds with the C9-methyl group (2, 4), the sulfonyl derivatives (IIa-2/4 and IIb-2/4) possess higher energy barriers compared with the corresponding benzoyl derivatives (I-2/4), which may be explained by the large steric hindrance to the flipping of the diazepine ring in the sulfonyl derivatives (IIa-2/4 and IIb-2/4) due to the rigidly folded conformation. The extraordinarily high energy barrier to isomerization in IIa-2 and IIb-2 (X = C=O, Y = CH₃) with the ΔG^\ddagger value of 132 kJ/mol (isomerization was almost negligible at 80 °C after 8 h), and the large energy differences of IIa-2 vs IIa-4 and IIb-2 vs IIb-4 (both Δ 27 kJ/mol) compared with that of I-2 vs I-4 (Δ 8 kJ/mol) are also of

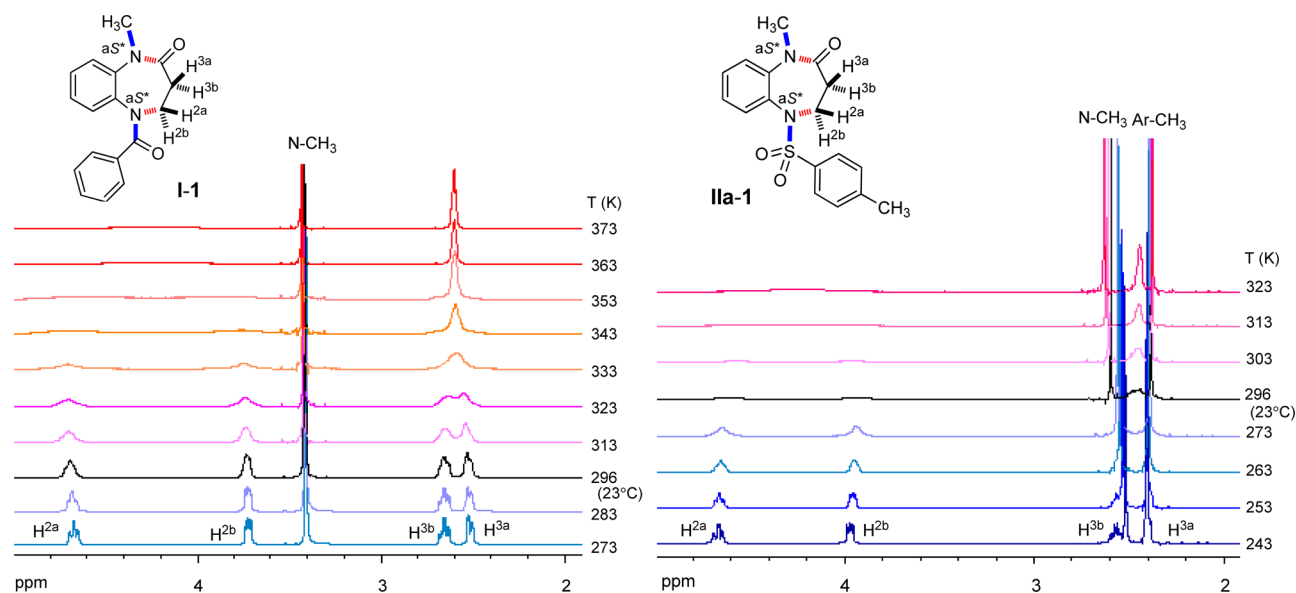


Figure 10. VT NMR spectra of I-1 (in $\text{CDCl}_2\text{CDCl}_2$) and IIa-1 (in CDCl_3).

particular interest. The extraordinarily high energy barrier observed in IIa-2/IIb-2 may be caused by the double effects of the lactam-ring structure and the folded conformations, which induce the highly rigid steric structure.

CONCLUSION

The atropisomerism caused by the $\text{Ar-N}(\text{SO}_2)$ axis of *N*-sulfonyl-1,5-benzodiazepines (IIa/b) was investigated in detail by comparing it with that caused by the $\text{Ar-N}(\text{CO})$ axis of the *N*-benzoyl congeners (I). The stable conformation of IIa/b was shown to be different from that of I by X-ray crystal structure analysis, ^1H NMR study, and computational study. The substituent (*p*-tolyl/methyl group) in the sulfonyl moiety of IIa/b occupies the position over the diazepine-ring (folded form), whereas that of I is *anti* to the diazepine-ring (extended form). The stereochemical stability also differed between the two congeners, and an extraordinarily high energy barrier to atropisomerization ($\Delta G^\ddagger = 132$ kJ/mol) observed in *N*-tosyl- and *N*-mesyl-1,5-benzodiazepin-2-ones (IIa-2 and IIb-2) was noteworthy, which may be caused by the double effects of the lactam-ring structure and the folded conformation. We hope that this study provides useful information not only on sulfonamide chemistry but also for future drug design.

EXPERIMENTAL SECTION²⁰

Preparation of *N*-Benzoyl-1,5-benzodiazepines (I) (1–4). 5-Benzoyl-1-methyl-1,3,4,5-tetrahydro-2*H*-1,5-benzodiazepin-2-one (I-1). Sodium hydride (60% in oil) (34 mg, 0.85 mmol) was added to a stirred solution of 1-methyl-1,3,4,5-tetrahydro-2*H*-1,5-benzodiazepin-2-one^{3f} (S1) (100 mg, 0.56 mmol) in THF (6 mL) at 0 °C under an argon atmosphere. The mixture was stirred at 25 °C for 30 min, cooled to 0 °C, and treated with benzoyl chloride (0.13 mL, 1.1 mmol). After being stirred at 25 °C for 1 h, the mixture was treated with H_2O and then extracted with ethyl acetate. The extract was washed with brine, dried, and concentrated. The concentrate was purified by column chromatography (silica gel, ethyl acetate/hexane = 1:2) to afford I-1 as colorless crystals (134 mg, 0.48 mmol, 84%): mp 108–110 °C; ^1H NMR (400 MHz, CDCl_3) δ 2.62–2.71 (m, 2H), 3.49 (s, 3H), 3.82 (br, 1H), 4.78 (br, 1H), 6.74 (br, 1H), 6.94 (br, 1H), 7.18–7.26 (m, 7H); ^{13}C NMR (100 MHz, CDCl_3) δ 33.3, 34.9, 49.9, 122.6, 126.4, 127.8, 128.2, 128.4, 130.1, 130.2, 135.1, 135.3, 140.6, 170.8, 171.1; IR

(KBr) 3060, 1671, 1647 cm^{-1} ; HRMS (ESI) m/z calcd for $\text{C}_{17}\text{H}_{16}\text{N}_2\text{O}_2$ 281.1285 ($\text{M} + \text{H}^+$), found 281.1279.

Compounds I-2, I-3, and I-4 were prepared from the corresponding 1,5-benzodiazepines (S2, S3, and S4) according to a similar procedure described for the preparation of I-1 from S1. Compound I-2 showed peaks of a mixture of *cis*- and *trans*-conformers (*cis/trans* = 10:1) in the ^1H NMR spectrum, whereas I-1, I-3, and I-4 showed only those of the *cis*-conformer at room temperature.

5-Benzoyl-1,6-dimethyl-1,3,4,5-tetrahydro-2*H*-1,5-benzodiazepin-2-one (I-2). Colorless crystals (91%): mp 135–137 °C; signals of a mixture of *cis/trans* (= 10:1) conformers were observed in the ^1H and ^{13}C NMR spectra; *cis*-conformer, ^1H NMR (600 MHz, CDCl_3) δ 1.97 (s, 3H), 2.57 (ddd, $J = 1.3, 5.8, 13.4$ Hz, 1H), 2.63 (ddd, $J = 6.8, 13.4, 13.7$ Hz, 1H), 3.51 (s, 3H), 3.65 (ddd, $J = 1.3, 6.8, 12.7$ Hz, 1H), 4.94 (ddd, $J = 5.8, 12.7, 13.7$ Hz, 1H), 6.86 (d, $J = 7.7$ Hz, 1H), 7.11–7.27 (m, 7H); ^{13}C NMR (100 MHz, CDCl_3) δ 18.0, 33.5, 34.8, 48.2, 120.1, 127.4, 127.9, 128.4, 128.6, 130.3, 133.9, 135.0, 136.8, 141.7, 170.1, 171.1; *trans*-conformer (only the distinguishable peaks are described), ^1H NMR δ 2.32 (dd, $J = 5.2, 13.1$ Hz, 1H \times 1/10), 2.38 (s, 3H \times 1/10), 3.37 (s, 3H \times 1/10), 3.73 (dd, $J = 7.2, 12.7$ Hz, 1H \times 1/10), 4.31 (ddd, $J = 5.8, 12.7, 13.1$ Hz, 1H \times 1/10), 7.33–7.36 (m, 1H \times 1/10), 7.43–7.53 (m, 7H \times 1/10); ^{13}C NMR δ 17.6, 34.2, 35.0, 51.4, 121.0, 127.1, 128.5, 128.6, 128.7, 130.2, 132.5, 135.2, 137.4, 142.1, 170.3, 170.4; IR (KBr) 3065, 1669 cm^{-1} ; HRMS (ESI) m/z calcd for $\text{C}_{18}\text{H}_{18}\text{N}_2\text{O}_2$ 295.1441 ($\text{M} + \text{H}^+$), found 295.1442.

1-Benzoyl-5-methyl-2,3,4,5-tetrahydro-1*H*-1,5-benzodiazepine (I-3): colorless oil (97%); ^1H NMR (600 MHz, CDCl_3) δ 1.84 (m, 1H), 2.10 (m, 1H), 2.83 (m, 1H), 2.97 (s, 3H), 3.13 (m, 1H), 3.47 (m, 1H), 4.66 (m, 1H), 6.55–6.59 (m, 2H), 6.92 (d, $J = 8.3$ Hz, 1H), 7.08–7.11 (m, 3H), 7.16–7.20 (m, 3H); ^{13}C NMR (150 MHz, CDCl_3) δ 26.8, 42.3, 45.2, 54.4, 117.6, 121.0, 127.6, 128.0, 128.2, 129.4, 129.6, 134.9, 136.5, 149.5, 170.2; IR (KBr) 2943, 1635 cm^{-1} ; HRMS (ESI) m/z calcd for $\text{C}_{17}\text{H}_{18}\text{N}_2\text{O}$ 267.1492 ($\text{M} + \text{H}^+$), found 267.1481.

1-Benzoyl-5,9-dimethyl-2,3,4,5-tetrahydro-1*H*-1,5-benzodiazepine (I-4). Colorless crystals (89%): mp 113–114 °C; ^1H NMR (600 MHz, CDCl_3) δ 1.71–1.77 (m, 1H), 1.91 (s, 3H), 2.07–2.13 (m, 1H), 2.81 (ddd, $J = 3.3, 8.1, 12.2$ Hz, 1H), 2.95 (s, 3H), 2.96–2.98 (m, 1H), 3.42 (ddd, $J = 3.5, 8.6, 12.2$ Hz, 1H), 4.70 (ddd, $J = 4.4, 8.7, 13.2$ Hz, 1H), 6.52 (d, $J = 7.7$ Hz, 1H), 6.79 (d, $J = 7.7$ Hz, 1H), 7.03 (t, $J = 7.7$ Hz, 1H), 7.07 (t, $J = 7.7$ Hz, 2H), 7.18 (t, $J = 7.4$ Hz, 1H), 7.24–7.26 (m, 2H); ^{13}C NMR (100 MHz, CDCl_3) δ 18.0, 26.5, 42.3, 44.0, 54.6, 115.1, 123.3, 127.0, 127.3, 128.1, 129.4, 133.5, 135.5, 136.3, 148.5, 167.9; IR (KBr) 2941, 1633 cm^{-1} ; HRMS (ESI) m/z calcd for $\text{C}_{18}\text{H}_{20}\text{N}_2\text{O}$ 281.1648 ($\text{M} + \text{H}^+$), found 281.1649.

Preparation of *N*-*p*-Tosyl-1,5-benzodiazepines (IIa) (1–4). 1-Methyl-5-(*p*-toluenesulfonyl)-1,3,4,5-tetrahydro-2H-1,5-benzodiazepin-2-one (IIa-1). To a stirred solution of S1 (13.5 mg, 0.078 mmol) in dichloromethane (1 mL) at 0 °C under argon were added triethylamine (53 mL, 0.077 mmol), DMAP (4.7 mg, 0.038 mmol), and *p*-toluenesulfonyl chloride (43.8 mg, 0.23 mmol). After being stirred at 25 °C for 4 h, the mixture was treated with H₂O and extracted with dichloromethane. The extract was dried and concentrated. The concentrate was purified by column chromatography (silica gel, ethyl acetate/hexane = 1/4) to afford IIa-1 as white powder (22.9 mg, 0.069 mmol, 91%): mp 177–179 °C; ¹H NMR (400 MHz, CDCl₃) δ 2.38 (s, 3H), 2.45 (br, 2H), 2.59 (s, 3H), 3.95 (br, 1H), 4.56 (br, 1H), 7.06 (dd, *J* = 1.4, 7.8 Hz, 1H), 7.24 (d, *J* = 8.0 Hz, 2H), 7.29 (dt, *J* = 1.4, 7.8 Hz, 1H), 7.39 (dt, *J* = 1.4, 7.8 Hz, 1H), 7.47 (d, *J* = 8.3 Hz, 2H), 7.63 (dd, *J* = 1.4, 7.8 Hz, 1H); ¹³C NMR (100 MHz, CDCl₃) δ 21.5, 34.0, 34.2, 51.7, 122.6, 126.5, 126.9, 129.4, 129.5, 130.3, 132.9, 137.1, 142.5, 143.3, 170.1; IR (KBr) 2946, 1671, 1341, 1158 cm⁻¹; HRMS (ESI) *m/z* calcd for C₁₇H₁₈N₂O₃S 331.1111 (M + H)⁺, found 331.1115.

1,6-Dimethyl-5-(*p*-toluenesulfonyl)-1,3,4,5-tetrahydro-2H-1,5-benzodiazepin-2-one (IIa-2). To a stirred solution of 1,6-dimethyl-1,3,4,5-tetrahydro-2H-1,5-benzodiazepin-2-one (S2) (15 mg, 0.079 mmol) in pyridine (2 mL) at 0 °C under argon were added DMAP (4.8 mg, 0.039 mmol) and *p*-toluenesulfonyl chloride (75 mg, 0.39 mmol). After the mixture was stirred at 25 °C for 28 h, the solvent was evaporated. To the residue were added H₂O and ethyl acetate, and the mixture was extracted with ethyl acetate. The extract was dried and concentrated. The concentrate was purified by column chromatography (silica gel, ethyl acetate/hexane = 1:3) to afford IIa-2 as pale yellow crystals (25 mg, 0.073 mmol, 92%): mp 186–188 °C; ¹H NMR (400 MHz, CDCl₃) δ 2.32 (ddd, *J* = 0.9, 5.3, 13.4 Hz, 1H), 2.44 (ddd, *J* = 7.0, 13.4, 13.6 Hz, 1H), 2.41 (s, 3H), 2.52 (s, 3H), 2.58 (s, 3H), 3.84 (ddd, *J* = 0.9, 7.0, 13.4 Hz, 1H), 4.57 (ddd, *J* = 5.3, 13.4, 13.6 Hz, 1H), 6.92 (dd, *J* = 0.9, 7.5 Hz, 1H), 7.21 (d, *J* = 7.0 Hz, 1H), 7.27–7.31 (m, 3H), 7.56 (d, *J* = 8.3 Hz, 2H); ¹³C NMR (100 MHz, CDCl₃) δ 19.3, 21.5, 34.2, 34.3, 50.7, 120.1, 127.1, 128.8, 129.1, 129.6, 129.6, 137.6, 142.4, 143.3, 143.6, 169.7; IR (KBr) 2928, 1667, 1339, 1155 cm⁻¹; HRMS (ESI) *m/z* calcd for C₁₈H₂₀N₂O₃S 345.1267 (M + H)⁺, found 345.1272.

Compounds IIa-3 and IIa-4 were prepared from the corresponding 1,5-benzodiazepines (S3 and S4)^{3f} according to similar procedures described for the preparation of IIa-1 from S1 and IIa-2 from S2, respectively.

5-Methyl-1-(*p*-toluenesulfonyl)-2,3,4,5-tetrahydro-1H-1,5-benzodiazepine (IIa-3). Colorless crystals (81%): mp 80–82 °C; ¹H NMR (600 MHz, CDCl₃) δ 1.74 (br, 2H), 2.36 (s, 3H), 2.37 (s, 3H), 2.71 (br, 2H), 3.72 (br, 2H), 6.78 (dd, *J* = 0.9, 8.2 Hz, 1H), 6.94 (dt, *J* = 1.4, 7.8 Hz, 1H), 7.15 (d, *J* = 8.2 Hz, 2H), 7.23 (dt, *J* = 1.9, 7.8 Hz, 1H), 7.41 (dd, *J* = 1.9, 7.8 Hz, 1H), 7.45 (d, *J* = 8.2 Hz, 2H); ¹³C NMR (150 MHz, CDCl₃) δ 21.4, 26.6, 41.2, 47.8, 53.5, 118.0, 121.1, 127.4, 128.7, 129.0, 130.3, 131.7, 137.9, 142.5, 148.5; IR (KBr) 1325, 1142 cm⁻¹; HRMS (ESI) *m/z* calcd for C₁₇H₂₀N₂O₂S 317.1318 (M + H)⁺, found 317.1337.

5,9-Dimethyl-1-(*p*-toluenesulfonyl)-2,3,4,5-tetrahydro-1H-1,5-benzodiazepine (IIa-4). Colorless crystals (96%): mp 96–98 °C; ¹H NMR (600 MHz, CDCl₃) δ 1.42–1.50 (m, 1H), 1.73–1.79 (m, 1H), 2.23 (s, 3H), 2.39 (s, 3H), 2.39–2.44 (m, 1H), 2.47 (s, 3H), 2.59 (ddd, *J* = 2.7, 9.6, 11.7 Hz, 1H), 3.29 (ddd, *J* = 5.0, 5.0, 13.3 Hz, 1H), 4.02 (ddd, *J* = 4.1, 9.3, 13.3 Hz, 1H), 6.62 (d, *J* = 7.5 Hz, 1H), 6.88 (d, *J* = 7.5 Hz, 1H), 7.14 (t, *J* = 7.5 Hz, 1H), 7.19 (d, *J* = 7.5 Hz, 2H), 7.54 (d, *J* = 8.3 Hz, 2H); ¹³C NMR (150 MHz, CDCl₃) δ 19.2, 21.5, 25.7, 40.8, 46.5, 53.2, 115.5, 123.7, 127.8, 128.6, 128.8, 138.6, 141.3, 142.3, 149.1; IR (KBr) 1336, 1156 cm⁻¹; HRMS (ESI) *m/z* calcd for C₁₈H₂₂N₂O₂S 331.1475 (M + H)⁺, found 331.1502.

Preparation of *N*-Methanesulfonyl-1,5-benzodiazepines (IIb) (1–4). 5-Methanesulfonyl-1-methyl-1,3,4,5-tetrahydro-2H-1,5-benzodiazepin-2-one (IIb-1). To a stirred solution of S1 (20.4 mg, 0.12 mmol) in pyridine (1.2 mL) at 0 °C under argon were added DMAP (7.1 mg, 0.058 mmol) and methanesulfonyl chloride (45 mL, 0.58 mmol). After the mixture was stirred at 25 °C for 28 h, the

solvent was evaporated. To the residue were added H₂O and ethyl acetate, and the mixture was extracted with ethyl acetate. The extract was washed with H₂O, dried, and concentrated. The concentrate was purified by column chromatography (silica gel, ethyl acetate/hexane = 1:2) to afford IIb-1 as colorless crystals (16 mg, 0.063 mmol, 54%): mp 119–121 °C; ¹H NMR (400 MHz, CDCl₃) δ 2.57 (br, 2H), 2.84 (s, 3H), 3.35 (s, 3H), 4.17 (br, 2H), 7.26–7.32 (m, 2H), 7.45 (dt, *J* = 1.4, 7.8 Hz, 1H), 7.52 (dd, *J* = 1.4, 7.8 Hz, 1H); ¹³C NMR (100 MHz, CDCl₃) δ 34.1, 35.0, 39.1, 51.3, 123.0, 127.0, 129.8, 130.7, 132.6, 142.5, 170.8; IR (KBr) 2927, 1663, 1336, 1156 cm⁻¹; HRMS (ESI) *m/z* calcd for C₁₁H₁₄N₂O₃S 255.0798 (M + H)⁺, found 255.0797.

Compounds IIb-2, IIb-3, and IIb-4 were prepared from the corresponding 1,5-benzodiazepines (S2, S3, and S4)^{3f} according to a similar procedure described for the preparation of IIb-1 from S1.

1,6-Dimethyl-5-methanesulfonyl-1,3,4,5-tetrahydro-2H-1,5-benzodiazepin-2-one (IIb-2). Colorless crystals (47%): mp 168–169 °C; ¹H NMR (400 MHz, CDCl₃) δ 2.46 (ddd, *J* = 0.9, 5.3, 13.4 Hz, 1H), 2.46 (s, 3H), 2.58 (ddd, *J* = 7.3, 13.4, 13.4 Hz, 1H), 2.87 (s, 3H), 3.35 (s, 3H), 3.79 (ddd, *J* = 0.9, 7.3, 13.4 Hz, 1H), 4.41 (ddd, *J* = 5.3, 13.4, 13.4 Hz, 1H), 7.10 (dd, *J* = 0.9, 7.8 Hz, 1H), 7.21 (dd, *J* = 0.9, 7.8 Hz, 1H), 7.33 (t, *J* = 7.8 Hz, 1H); ¹³C NMR (100 MHz, CDCl₃) δ 19.0, 34.3, 34.9, 39.3, 50.3, 120.5, 129.1, 129.4, 130.1, 142.0, 143.2, 170.8; IR (KBr) 2928, 1654, 1335, 1149 cm⁻¹; HRMS (ESI) *m/z* calcd for C₁₂H₁₆N₂O₃S 269.0954 (M + H)⁺, found 269.0954.

1-(Methanesulfonyl)-5-methyl-2,3,4,5-tetrahydro-1H-1,5-benzodiazepine (IIb-3). Colorless crystals (91%): mp 112 °C; ¹H NMR (600 MHz, CDCl₃) δ 1.88 (br, 2H), 2.86 (s, 3H), 2.87 (s, 3H), 2.98 (br, 2H), 3.69 (br, 2H), 7.00 (dt, *J* = 1.8, 8.3 Hz, 2H), 7.29 (dt, *J* = 1.8, 8.3 Hz, 1H), 7.41 (dd, *J* = 1.8, 7.8 Hz, 1H); ¹³C NMR (150 MHz, CDCl₃) δ 27.5, 39.8, 42.2, 47.7, 54.6, 118.2, 122.3, 129.4, 131.1, 132.1, 149.1; IR (KBr) 1322, 1155 cm⁻¹; HRMS (ESI) *m/z* calcd for C₁₁H₁₆N₂O₂S 241.1005 (M + H)⁺, found 241.0996.

5,9-Dimethyl-1-(methanesulfonyl)-2,3,4,5-tetrahydro-1H-1,5-benzodiazepine (IIb-4). Colorless crystals (71%): mp 116 °C; ¹H NMR (600 MHz, CDCl₃) δ 1.56–1.63 (m, 1H), 2.02–2.09 (m, 1H), 2.42 (s, 3H), 2.67 (ddd, *J* = 3.4, 8.3, 11.6 Hz, 1H), 2.82 (s, 3H), 2.95 (s, 3H), 3.16–3.23 (m, 2H), 4.11 (ddd, *J* = 4.6, 8.1, 13.8 Hz, 1H), 6.86 (d, *J* = 7.8 Hz, 1H), 6.93 (d, *J* = 7.8 Hz, 1H), 7.18 (t, *J* = 7.8 Hz, 1H); ¹³C NMR (150 MHz, CDCl₃) δ 19.2, 26.8, 40.3, 41.8, 46.8, 54.6, 115.8, 124.9, 129.0, 129.9, 141.2, 149.8; IR (KBr) 1325, 1153 cm⁻¹; HRMS (ESI) *m/z* calcd for C₁₂H₁₈N₂O₂S 255.1162 (M + H)⁺, found 255.1158.

Separation of the *N*-Benzoyl- and *N*-Sulfonyl-1,5-benzodiazepines into the Atropisomers using Chiral HPLC. Atropisomers of 5-Benzoyl-1,6-dimethyl-1,3,4,5-tetrahydro-2H-1,5-benzodiazepin-2-one (aR-I-2 and aS-I-2).^{3f} CHIRALPAK IA (1.0 cm ϕ × 25 cm); eluent, hexane/ethanol (19:1); Flow rate, 3.0 mL/min; temperature, 25 °C; detection, 254 nm. Former peak (aR-I-2): retention time = 53.6 min; [α]_D²³ –115.0 (c 0.11, MeOH). Latter peak (aS-I-2): retention time = 67.2 min; [α]_D²³ +113.1 (c 0.11, MeOH). ¹H NMR spectra of the enantiomers were the same as that of the racemate (I-2). The absolute stereochemistry of the separated atropisomers of I-2 was determined by the single-crystal X-ray analysis of both enantiomers.

Similarly, atropisomers of I-4, IIa-2, IIa-4, IIb-2, and IIb-4 were separated using chiral HPLC.

Atropisomers of 5-Benzoyl-1,6-dimethyl-2,3,4,5-tetrahydro-1H-1,5-benzodiazepine (aR-I-4 and aS-I-4).^{3f} CHIRALPAK IA (1.0 cm ϕ × 25 cm); eluent, hexane/2-propanol (19:1); flow rate, 1.5 mL/min; temperature, 25 °C; detection, 254 nm. Former peak (aS-I-4): retention time = 28.6 min; [α]_D²³ +151.0 (c 0.11, MeOH). Latter peak (aR-I-4): retention time = 35.6 min; [α]_D²³ –146.7 (c 0.11, MeOH). The absolute stereochemistry of the separated atropisomers of I-4 was determined by the single-crystal X-ray analysis of aS-I-4.

Atropisomers of 1,6-Dimethyl-5-(*p*-toluenesulfonyl)-1,3,4,5-tetrahydro-2H-1,5-benzodiazepin-2-one (aS-IIa-2 and aR-IIa-2). CHIRALPAK IA (1.0 cm ϕ × 25 cm); eluent, hexane/ethanol (9:1); flow rate, 2.5 mL/min; temperature, 24 °C; detection, 254 nm. Former peak (aS-IIa-2): retention time = 27.7 min; [α]_D²² –155.2 (c 0.295,

MeOH). Latter peak, (aR-*Ila-2*): retention time = 38.4 min; $[\alpha]_{D}^{22}$, +159.7 (c 0.29, MeOH).

Atropisomers of 5,9-Dimethyl-1-(p-toluenesulfonyl)-2,3,4,5-tetrahydro-1*H*-1,5-benzodiazepine (aS-*Ila-4* and aR-*Ila-4*). CHIRALPAK IA (1.0 cm ϕ \times 25 cm); eluent, hexane/2-propanol (19:1); flow rate, 2.0 mL/min; temperature, 23 °C; detection, 254 nm. Former peak (aS-*Ila-4*): retention time = 26.8 min; $[\alpha]_{D}^{20}$, -134.0 (c 0.115, MeOH). Latter peak (aR-*Ila-4*): retention time = 28.7 min; $[\alpha]_{D}^{20}$, +136.6 (c 0.155, MeOH).

Atropisomers of 5-Methanesulfonyl-1,6-dimethyl-1,3,4,5-tetrahydro-2*H*-1,5-benzodiazepin-2-one (aS-*Iib-2* and aR-*Iib-2*). CHIRALPAK IA (1.0 cm ϕ \times 25 cm); eluent, hexane/ethanol (9:1); flow rate, 2.5 mL/min; temperature, 24 °C; detection, 254 nm. Former peak (aS-*Iib-2*): retention time = 44.6 min; $[\alpha]_{D}^{20}$, -159.2 (c 0.13, MeOH). Latter peak (aR-*Iib-2*): retention time = 47.6 min; $[\alpha]_{D}^{20}$, +164.1 (c 0.13, MeOH).

Atropisomers of 5,9-Dimethyl-1-methanesulfonyl-2,3,4,5-tetrahydro-1*H*-1,5-benzodiazepine (aS-*Iib-4* and aR-*Iib-4*). CHIRALPAK IA (1.0 cm ϕ \times 25 cm); eluent, hexane/ethanol (19:1); flow rate, 2.0 mL/min; temperature, 23 °C; detection, 254 nm. Former peak (aR-*Iib-4*): retention time = 30.4 min; $[\alpha]_{D}^{20}$, +81.4 (c 0.055, MeOH). Latter peak (aS-*Iib-4*): retention time = 33.7 min; $[\alpha]_{D}^{20}$, -88.5 (c 0.06, MeOH).

X-ray Crystallographic Data. Crystal Data of aR-*I-2* (CCDC 803349). $C_{18}H_{18}O_2N_2$; mp 135–137 °C, M_r = 294.35, Cu $K\alpha$ (λ = 1.54187 Å), orthorhombic, $P2_12_12_1$, colorless prism 0.25 \times 0.20 \times 0.15 mm, crystal dimensions a = 9.9010(5) Å, b = 10.9880(4) Å, c = 14.389(12) Å, α = 90°, β = 90°, γ = 90°, T = 173 K, Z = 4, V = 1565.41(12) Å³, D_{calc} = 1.249 g cm⁻³, μ Cu $K\alpha$ = 6.613 cm⁻¹, F_{000} = 624.00, GOF = 1.278, R_{int} = 0.022, R_1 = 0.0261, wR_2 = 0.0573, Flack parameter = -0.08 (19).

Crystal Data of aS-*I-2* (CCDC 803350). $C_{18}H_{18}O_2N_2$; mp 135–137 °C, M_r = 294.35, Cu $K\alpha$ (λ = 1.54187 Å), orthorhombic, $P2_12_12_1$, colorless prism 0.30 \times 0.20 \times 0.15 mm, crystal dimensions a = 9.9005(3) Å, b = 10.9852(3) Å, c = 14.3892(5) Å, α = 90°, β = 90°, γ = 90°, T = 173 K, Z = 4, V = 1564.96(9) Å³, D_{calc} = 1.249 g cm⁻³, μ Cu $K\alpha$ = 6.614 cm⁻¹, F_{000} = 624.00, GOF = 0.660, R_{int} = 0.061, R_1 = 0.0424, wR_2 = 0.1002, Flack parameter = 0.1 (4).

Crystal Data of aS-*I-4* (CCDC 803351). $C_{18}H_{20}ON_2$; mp 113–114 °C, M_r = 280.37, Cu $K\alpha$ (λ = 1.54187 Å), orthorhombic, $P2_12_12_1$, colorless prism 0.25 \times 0.15 \times 0.10 mm, crystal dimensions a = 8.5018(5) Å, b = 10.0616(6) Å, c = 18.1012(9) Å, α = 90°, β = 90°, γ = 90°, T = 173 K, Z = 4, V = 1548.40(15) Å³, D_{calc} = 1.203 g cm⁻³, μ Cu $K\alpha$ = 5.899 cm⁻¹, F_{000} = 600.00, GOF = 0.734, R_{int} = 0.045, R_1 = 0.0406, wR_2 = 0.0937, Flack parameter = 0.0 (4).

Crystal Data of aR-*Ila-2* (CCDC 995609). $C_{18}H_{20}N_2O_3S$; mp 183–184 °C, M_r = 344.43, Cu $K\alpha$ (λ = 1.54187 Å), orthorhombic, $P2_12_12_1$, colorless prism 0.20 \times 0.20 \times 0.10 mm, crystal dimensions a = 6.5380(2) Å, b = 13.6252(3) Å, c = 18.5986(4) Å, α = 90°, β = 90°, γ = 90°, T = 173 K, Z = 4, V = 1295.96(5) Å³, D_{calc} = 1.381 g cm⁻³, μ Cu $K\alpha$ = 18.980 cm⁻¹, F_{000} = 728.00, GOF = 1.118, R_{int} = 0.0343, R_1 = 0.0331, wR_2 = 0.0942, Flack parameter = -0.007 (17).

Crystal Data of *Ila-3* (CCDC 995610). $C_{17}H_{20}N_2O_2S$; mp 80–82 °C, M_r = 316.42, Cu $K\alpha$ (λ = 1.54187 Å), triclinic, $P-1$, colorless prism 0.200 \times 0.100 \times 0.050 mm, crystal dimensions a = 7.7090(3) Å, b = 8.0411(2) Å, c = 13.5247(4) Å, α = 80.148(2)°, β = 89.037(2)°, γ = 76.394(2)°, T = 173 K, Z = 2, V = 802.60(4) Å³, D_{calc} = 1.309 g cm⁻³, μ Cu $K\alpha$ = 18.604 cm⁻¹, F_{000} = 336.00, GOF = 3.360, R_{int} = 0.0311, R_1 = 0.0544, wR_2 = 0.1241.

Crystal Data of aS-*Ila-4* (CCDC 995611). $C_{18}H_{22}N_2O_2S$; mp 98–99 °C, M_r = 330.44, Cu $K\alpha$ (λ = 1.54187 Å), orthorhombic, $P2_12_12_1$, colorless prism 0.250 \times 0.200 \times 0.150 mm, crystal dimensions a = 7.8482(2) Å, b = 8.2682(2) Å, c = 26.3414(5) Å, α = 90°, β = 90°, γ = 90°, T = 173 K, Z = 4, V = 1709.30(7) Å³, D_{calc} = 1.284 g cm⁻³, μ Cu $K\alpha$ = 17.685 cm⁻¹, F_{000} = 704.00, GOF = 1.112, R_{int} = 0.0266, R_1 = 0.0323, wR_2 = 0.0915, Flack parameter = 0.009 (16).

Crystal Data of aR-*Ila-4* (CCDC 995612). $C_{18}H_{22}N_2O_2S$; mp 100–102 °C, M_r = 330.44, Cu $K\alpha$ (λ = 1.54187 Å), orthorhombic, $P2_12_12_1$, colorless prism 0.100 \times 0.100 \times 0.050 mm, crystal dimensions a = 7.8482(3) Å, b = 8.2717(3) Å, c = 26.3382(7) Å, α = 90°, β = 90°, γ

90°, T = 173 K, Z = 4, V = 1709.83(9) Å³, D_{calc} = 1.284 g cm⁻³, μ Cu $K\alpha$ = 17.679 cm⁻¹, F_{000} = 704.00, GOF = 1.709, R_{int} = 0.0395, R_1 = 0.0625, wR_2 = 0.1712, Flack parameter = 0.03 (3).

Crystal Data of *Iib-1* (CCDC 995613). $C_{11}H_{14}N_2O_3S$; mp 119–121 °C, M_r = 254.30, Cu $K\alpha$ (λ = 1.54187 Å), triclinic, $P-1$, colorless prism 0.20 \times 0.20 \times 0.15 mm, crystal dimensions a = 7.9089(2) Å, b = 8.8674(3) Å, c = 9.2796(3) Å, α = 83.012(2)°, β = 69.906(2)°, γ = 75.185(2)°, T = 173 K, Z = 2, V = 590.45(3) Å³, D_{calc} = 1.430 g cm⁻³, μ Cu $K\alpha$ = 24.482 cm⁻¹, F_{000} = 268.00, GOF = 1.661, R_{int} = 0.0259, R_1 = 0.0404, wR_2 = 0.1295.

Crystal Data of *Iib-2* (CCDC 995614). $C_{12}H_{16}N_2O_3S$; mp 168–169 °C, M_r = 268.33, Cu $K\alpha$ (λ = 1.54187 Å), monoclinic, $P2_1/c$, colorless prism 0.20 \times 0.15 \times 0.10 mm, crystal dimensions a = 7.5366(1) Å, b = 24.0628(4) Å, c = 7.4528(1) Å, α = 90°, β = 111.9550°, γ = 90°, T = 173 K, Z = 4, V = 1295.96(5) Å³, D_{calc} = 1.422 g cm⁻³, μ Cu $K\alpha$ = 23.354 cm⁻¹, F_{000} = 568.00, GOF = 1.320, R_{int} = 0.0232, R_1 = 0.0379, wR_2 = 0.1116.

Crystal Data of aS-*Iib-2* (CCDC 995615). $C_{12}H_{16}N_2O_3S$; mp 145–146 °C, M_r = 268.33, Cu $K\alpha$ (λ = 1.54187 Å), orthorhombic, $P2_12_12_1$, colorless prism 0.25 \times 0.20 \times 0.10 mm, crystal dimensions a = 6.5509(2) Å, b = 8.5910(2) Å, c = 23.0273(5) Å, α = 90°, β = 90°, γ = 90°, T = 173 K, Z = 4, V = 1295.96(5) Å³, D_{calc} = 1.375 g cm⁻³, μ Cu $K\alpha$ = 22.590 cm⁻¹, F_{000} = 568.00, GOF = 1.050, R_{int} = 0.0407, R_1 = 0.0330, wR_2 = 0.0881, Flack parameter = -0.006 (19).

Crystal Data of *Iib-3* (CCDC 995616). $C_{11}H_{16}N_2O_2S$; mp 112 °C, M_r = 240.32, Cu $K\alpha$ (λ = 1.54187 Å), triclinic, $P-1$, colorless prism 0.100 \times 0.100 \times 0.050 mm, crystal dimensions a = 7.9146(3) Å, b = 8.8541(3) Å, c = 9.1732(3) Å, α = 104.507(2)°, β = 95.734(2)°, γ = 110.408(2)°, T = 173 K, Z = 2, V = 570.72(3) Å³, D_{calc} = 1.398 g cm⁻³, μ Cu $K\alpha$ = 24.263 cm⁻¹, F_{000} = 256.00, GOF = 1.520, R_{int} = 0.0294, R_1 = 0.0386, wR_2 = 0.1344.

Crystal Data of aS-*Iib-4* (CCDC 995617). $C_{12}H_{18}N_2O_2S$; mp 129 °C, M_r = 254.35, Cu $K\alpha$ (λ = 1.54187 Å), orthorhombic, $P2_12_12_1$, colorless prism 0.200 \times 0.200 \times 0.050 mm, crystal dimensions a = 9.1979(2) Å, b = 10.6804(2) Å, c = 12.7106(3) Å, α = 90°, β = 90°, γ = 90°, T = 173 K, Z = 4, V = 1248.65(4) Å³, D_{calc} = 1.353 g cm⁻³, μ Cu $K\alpha$ = 22.472 cm⁻¹, F_{000} = 544.00, GOF = 1.837, R_{int} = 0.0404, R_1 = 0.0434, wR_2 = 0.0800, Flack parameter = 0.00 (3).

Crystal Data of aR-*Iib-4* (CCDC 995618). $C_{12}H_{18}N_2O_2S$; mp 128–129 °C, M_r = 254.35, Cu $K\alpha$ (λ = 1.54187 Å), orthorhombic, $P2_12_12_1$, colorless prism 0.200 \times 0.150 \times 0.100 mm, crystal dimensions a = 9.1971(3) Å, b = 10.6801(3) Å, c = 12.7121(3) Å, α = 90°, β = 90°, γ = 90°, T = 173 K, Z = 4, V = 1248.65(6) Å³, D_{calc} = 1.353 g cm⁻³, μ Cu $K\alpha$ = 22.472 cm⁻¹, F_{000} = 544.00, GOF = 1.105, R_{int} = 0.0339, R_1 = 0.0339, wR_2 = 0.0926, Flack parameter = 0.00 (2).

Stereochemical (Thermodynamic) Stability of Atropisomers [(aR)/(aS)-*I-2*, (aR)/(aS)-*I-4*, (aR)/(aS)-*Ila-2*, (aR)/(aS)-*Ila-4*, (aR)/(aS)-*Iib-2*, and (aR)/(aS)-*Iib-4*] (Determination of ΔG^\ddagger Value). To examine thermal stability of enantiomers, the time-dependent conversion rate (%) was estimated from chiral or nonchiral HPLC analysis of a solution of the diastereomers or enantiomer in toluene (or DMSO) after allowing to stand at designated temperatures. The ΔG^\ddagger value was determined according to a calculation method reported in a literature.¹⁸ The details including the figures of conversion profiles are shown in the Supporting Information.

COMPUTATIONAL METHODS

The conformational analyses for estimation of the stability of (aS)-*I-4* and (aS)-*Ila-4* were carried out by using the Gaussian 03 suites of programs.²¹ In the calculations of energy surfaces defined by two dihedral angles, all geometrical optimizations were performed using RHF/STO-3G level of theory. This basis set was set up to scan all conformations in the energy surfaces and reduce computational costs and times. To cover all conformational spaces, rotational steps of the two dihedral angles around single bonds in (aS)-*I-4* and (aS)-*Ila-4* were 15 degrees. During these ab initio calculations, all internal coordinates were optimized by the Berny algorithm and convergence of geometric optimization was tested against criteria for the maximum force component, root-mean-square force, maximum displacement component, and root-mean-square displacement. The obtained energy

surfaces are shown in Figures S1 and S2 (Supporting Information).¹⁷ Furthermore, to estimate the most stable conformation and the activation energies between stable conformers, fully geometry optimization of all equilibrium stable ($EQ_{a,b,1}$, $EQ_{a,b,2}$, $EQ_{a,b,3}$, $EQ_{a,b,4}$) and transition state ($TS_{a,b,1}$, $TS_{a,b,2}$, $TS_{a,b,3}$, $TS_{a,b,4}$, $TS_{b,5}$, $TS_{b,6}$) conformers extracted from the energy surfaces were carried out by using the RB3LYP density functional and the 6-31G(d) basis set (Figures S1 and S2, Supporting Information). The transition structures were obtained by the Synchronous Transit-Guided Quasi-Newton (STQN) method with QST3 option. Harmonic vibrational frequency analyses characterized the optimized structures (Table S1 and S2, Supporting Information).¹⁷

■ ASSOCIATED CONTENT

● Supporting Information

General experimental procedure; ¹H, ¹³C, and 2D (NOESY) NMR spectra for new compounds; VT NMR for **I-1**, **I-3**, **IIa-1**, **IIa-3**, **IIb-1**, and **IIb-3**; figures of thermal isomerization rate of atropisomers for (aR)/(aS)-**I-2**, (aR)/(aS)-**I-4**, (aR)/(aS)-**IIa-2**, (aR)/(aS)-**IIa-4**, (aR)/(aS)-**IIb-2**, and (aR)/(aS)-**IIb-4**; X-ray data (CIF) for (aR)-**IIa-2**, **IIa-3**, (aS)-**IIa-4**, (aR)-**IIa-4**, **IIb-1**, **IIb-2**, (aS)-**IIb-2**, **IIb-3**, (aR)-**IIb-4**, and (aS)-**IIb-4**; detailed calculation methods for (aS)-**I-4**, (aS)-**IIa-4**, (aS)-**IIb-2**, and (aS*)-**IIb-2**. This material is available free of charge via the Internet at <http://pubs.acs.org>.

■ AUTHOR INFORMATION

Corresponding Author

*E-mail: natsu@pharm.teikyo-u.ac.jp.

Notes

The authors declare no competing financial interest.

■ ACKNOWLEDGMENTS

This work was supported in part by a Grant-in-Aid for Scientific Research (C) (25460154) and a Grant-in-Aid for Young Scientists (B) (25860091) from the Japan Society for the Promotion of Sciences. We are grateful to Professor Takenori Kusumi (Tokyo Institute of Technology) for useful discussions on the NMR data.

■ REFERENCES

- (1) A recent review article on seven-membered-ring heterocycles, see: Ryan, J. H.; Hyland, C.; Meyer, A. G.; Smith, J. A.; Yin, J. X. *Prog. Heterocycl. Chem.* **2012**, *24*, 493–536.
- (2) For recent review articles on the relation between axial chirality and biological activity, see: (a) Clayden, J.; Moran, W. J.; Edwards, P. J.; LaPlante, S. R. *Angew. Chem., Int. Ed.* **2009**, *48*, 6398–6401. (b) LaPlante, S. R.; Edwards, P. J.; Fader, L. D.; Jakalian, A.; Hucke, O. *ChemMedChem* **2011**, *6*, 505–513. (c) LaPlante, S. R.; Fader, L. D.; Fandrick, K. R.; Fandrick, D. R.; Hucke, O.; Kemper, R.; Miller, S. P. F.; Edwards, P. J. *J. Med. Chem.* **2011**, *54*, 7005–7022. (d) Zask, A.; Murphy, J.; Ellestad, G. A. *Chirality* **2013**, *25*, 265–274. (e) Ramig, K. *Tetrahedron* **2013**, *69*, 10783–10795.
- (3) (a) Natsugari, H.; Ikeura, Y.; Kamo, I.; Ishimaru, T.; Ishichi, Y.; Fujishima, A.; Tanaka, T.; Kasahara, F.; Kawada, M.; Doi, T. *J. Med. Chem.* **1999**, *42*, 3982–3993. (b) Ishichi, Y.; Ikeura, Y.; Natsugari, H. *Tetrahedron* **2004**, *60*, 4481–4490. (c) Lee, S.; Kamide, T.; Tabata, H.; Takahashi, H.; Shiro, M.; Natsugari, H. *Bioorg. Med. Chem.* **2008**, *16*, 9519–9523. (d) Tabata, H.; Akiba, K.; Lee, S.; Takahashi, H.; Natsugari, H. *Org. Lett.* **2008**, *10*, 4871–4874. (e) Tabata, H.; Suzuki, H.; Akiba, K.; Takahashi, H.; Natsugari, H. *J. Org. Chem.* **2010**, *75*, 5984–5993. (f) Tabata, H.; Nakagomi, J.; Morizono, D.; Oshitari, T.; Takahashi, H.; Natsugari, H. *Angew. Chem., Int. Ed.* **2011**, *50*, 3075–3079. (g) Tabata, H.; Wada, N.; Takada, Y.; Oshitari, T.; Takahashi, H.; Natsugari, H. *J. Org. Chem.* **2011**, *76*, 5123–5131. (h) Tabata, H.; Wada, N.; Takada, Y.; Nakagomi, J.; Miike, T.; Shirahase, H.; Oshitari,

T.; Takahashi, H.; Natsugari, H. *Chem.–Eur. J.* **2012**, *18*, 1572–1576. (i) Tabata, H.; Yoneda, T.; Oshitari, T.; Takahashi, H.; Natsugari, H. *J. Org. Chem.* **2013**, *78*, 6264–6270.

(4) The terms aS and aR (chiral axis nomenclature) correspond to P and M (helix nomenclature), respectively.

(5) Ogawa, H.; Yamashita, H.; Kondo, K.; Yamamura, Y.; Miyamoto, H.; Kan, K.; Kitano, K.; Tanaka, M.; Nakaya, K.; Nakamura, S.; Mori, T.; Tominaga, M.; Yabuuchi, Y. *J. Med. Chem.* **1996**, *39*, 3547–3555.

(6) (a) Kondo, K.; Ogawa, H.; Yamashita, H.; Miyamoto, H.; Tanaka, M.; Nakaya, K.; Kitano, K.; Yamamura, Y.; Nakamura, S.; Onogawa, T.; Mori, T.; Tominaga, M. *Bioorg. Med. Chem.* **1999**, *7*, 1743–1757. (b) Ghali, J. K.; Hamad, B.; Yasothan, U.; Kirkpatrick, P. *Nat. Rev. Drug Discovery* **2009**, *8*, 611–612.

(7) Examples of biologically active compounds having a sulfonamide moiety: (a) Watanabe, M.; Koike, H.; Ishiba, T.; Okada, T.; Seo, S.; Hirai, K. *Bioorg. Med. Chem.* **1997**, *5*, 437–444. (b) Hunt, J. T.; Ding, C. Z.; Batorsky, R.; Bednarz, M.; Bhide, R.; Cho, Y.; Chong, S.; Chao, S.; Gullo-Brown, J.; Guo, P.; Kim, S. H.; Lee, F. Y. F.; Leftheris, K.; Miller, A.; Mitt, T.; Patel, M.; Penhallow, B. A.; Ricca, C.; Rose, W. C.; Schmidt, R.; Slusarchyk, W. A.; Vite, G.; Manne, V. *J. Med. Chem.* **2000**, *43*, 3587–3595. (c) Deur, C.; Agrawal, A. K.; Baum, H.; Booth, J.; Bove, S.; Brieland, J.; Bunker, A.; Connolly, C.; Cornicelli, J.; Dumin, J.; Finzel, B.; Gan, X.; Guppy, S.; Kamilar, G.; Kilgore, K.; Lee, P.; Loi, C.-M.; Lou, Z.; Morris, M.; Philippe, L.; Przybranowski, S.; Riley, F.; Samas, B.; Sanchez, B.; Tecle, H.; Wang, Z.; Welch, K.; Wilson, M.; Yates, K. *Bioorg. Med. Chem. Lett.* **2007**, *17*, 4599–4603. (d) Nishida, H.; Hasuoka, A.; Arikawa, Y.; Kurasawa, O.; Hirase, K.; Inatomi, N.; Hori, Y.; Sato, F.; Tarui, N.; Imanishi, A.; Kondo, M.; Takagi, T.; Kajino, M. *Bioorg. Med. Chem.* **2012**, *20*, 3925–3938. (e) Goswami, R.; Mukherjee, S.; Wohlfahrt, G.; Ghadiyaram, C.; Nagaraj, J.; Chandra, B. R.; Sistla, R. K.; Satyam, L. K.; Samiulla, D. S.; Moilanen, A.; Subramanya, H. S.; Ramachandra, M. *ACS Med. Chem. Lett.* **2013**, *4*, 1152–1157. (f) Meneyrol, J.; Follmann, M.; Lassalle, G.; Wehner, V.; Barre, G.; Rousseaux, T.; Altenburger, J.-M.; Petit, F.; Bocskei, Z.; Schreuder, H.; Alet, N.; Herault, J.-P.; Millet, L.; Dol, F.; Florian, P.; Schaeffer, P.; Sadoun, F.; Klieber, S.; Briot, C.; Bono, F.; Herbert, J.-M. *J. Med. Chem.* **2013**, *56*, 9441–9456.

(8) (a) Welch, C. J.; Gong, X.; Schafer, W. A.; Chobanian, H. R.; Lin, L. S.; Biba, M.; Liu, P.; Guo, Y.; Beard, A. *Chirality* **2009**, *21*, 105–109. (b) Liu, P.; Lanza, T. J., Jr.; Chiold, M.; Jones, C.; Chobanian, H. R.; Guo, Y.; Chang, L.; Kelly, T. M.; Kan, Y.; Palyha, O.; Guan, X.-M.; Marsh, D. J.; Metzger, J. M.; Ramsay, K.; Wang, S.-P.; Strack, A. M.; Miller, R.; Pang, J.; Lyons, K.; Dragovic, J.; Ning, J. G.; Schafer, W. A.; Welch, C. J.; Gong, X.; Gao, Y.-D.; Hornak, V.; Ball, R. G.; Tsou, N.; Reitman, M. L.; Wyratt, M. J.; Nargund, R. P.; Lin, L. S. *ACS Med. Chem. Lett.* **2011**, *2*, 933–937. (c) Chobanian, H. R.; Guo, Y.; Liu, P.; Chiold, M.; Lanza, T. J., Jr.; Chang, L.; Kelly, T. M.; Kan, Y.; Palyha, O.; Guan, X.-M.; Marsh, D. J.; Metzger, J. M.; Gorski, J. N.; Raustad, K.; Wang, S.-P.; Strack, A. M.; Miller, R.; Pang, J.; Madeira, M.; Lyons, K.; Dragovic, J.; Reitman, M. L.; Nargund, R. P.; Lin, L. S. *ACS Med. Chem. Lett.* **2012**, *3*, 252–256. (d) Chobanian, H. R.; Guo, Y.; Liu, P.; Lanza, T. J., Jr.; Chiold, M.; Chang, L.; Kelly, T. M.; Kan, Y.; Palyha, O.; Guan, X.-M.; Marsh, D. J.; Metzger, J. M.; Raustad, K.; Wang, S.-P.; Strack, A. M.; Gorski, J. N.; Miller, R.; Pang, J.; Lyons, K.; Dragovic, J.; Ning, J. G.; Schafer, W. A.; Welch, C. J.; Gong, X.; Gao, Y.-D.; Hornak, V.; Reitman, M. L.; Nargund, R. P.; Lin, L. S. *Bioorg. Med. Chem.* **2012**, *20*, 2845–2849.

(9) The absolute stereochemistry of MK-7725 is denoted as aR (chiral axis nomenclature), whereas the stereochemistry is alternatively denoted as pS according to the planar chirality nomenclature.^{8b}

(10) For convenience, the nitrogen replaced by the benzoyl and sulfonyl group was assigned no. 1 throughout the main text except for the compound names in the Experimental Section, although the numbering according to the nomenclature rule is different between the 1/2 (X = C=O) and 3/4 (X = CH₂) series of compounds.

(11) The *cis*- and *trans*-stereochemistry of **I-2** was assigned by comparing the chemical shifts of the methylene protons with those of the related compound (5-(*p*-chlorobenzoyl)-1,6-dimethyl-1,3,4,5-tetrahydro-2*H*-1,5-benzodiazepin-2-one), the stereochemistry of

which was supported by a NOESY experiment performed at $-30\text{ }^{\circ}\text{C}$; the aryl *o*-CH₃ group in the major *cis*-isomer showed a correlation peak to the protons of the benzoyl ring.^{3f}

(12) The absolute stereochemistry was determined based on the Flack parameter.

(13) Since the seven-membered ring is sufficiently small that the two axes move together like a gear during the ring flip,^{3d} the stereochemistry is specified to be the undistorted (*a*¹*R**, *a*²*R**) form, which was demonstrated by X-ray analysis of (*aR*)-**I-2** and (*aS*)-**I-2**.^{3f}

(14) Karplas, M. *J. Am. Chem. Soc.* **1963**, *85*, 2870–2871.

(15) The S–N single-bond distance is reported to be around 1.75 Å, see: Bharatam, P. V.; Gupta, A. A.; Kaur, D. *Tetrahedron* **2002**, *58*, 1759–1764.

(16) The folded form of **IIb-2** was supported by a computational study: i.e., the total energy difference between the conformations of (*aS**)-**IIb-2** (the folded form) and (–)-(*aS*)-**IIb-2** (the extended form) shown in Figure 6 was estimated by calculation using by RB3LYP/6-31G(d) to reveal the former is more stable than the latter by 7.5 kJ/mol (Table S2, Supporting Information).¹⁷

(17) For the detailed calculation results including the figures of the energy surface, and the tables of the total electronic energies, optimized geometries of stable equilibrium, and transition-state conformers, see the Supporting Information.

(18) For determination of ΔG^{\ddagger} values by VT NMR, see: Boiadjiev, S. E.; Lightner, D. A. *Tetrahedron* **2002**, *58*, 7411–7421. For the detailed variable-temperature ¹H NMR (VT NMR) spectra of **I-1/I-3**, **IIa-1/IIa-3**, and **IIb-1/IIb-3**, see the Supporting Information.

(19) For determination of ΔG^{\ddagger} values, see: Petit, M.; Lapierre, A. J. B.; Curran, D. P. *J. Am. Chem. Soc.* **2005**, *127*, 14994–14995.

(20) For general experimental methods, see the Supporting Information.

(21) Frisch, M. J.; Trucks, G. W.; Schlegel, H. B.; Scuseria, G. E.; Robb, M. A.; Cheeseman, J. R.; Montgomery, J. A., Jr.; Vreven, T.; Kudin, K. N.; Burant, J. C.; Millam, J. M.; Iyengar, S. S.; Tomasi, J.; Barone, V.; Mennucci, B.; Cossi, M.; Scalmani, G.; Rega, N.; Petersson, G. A.; Nakatsuji, H.; Hada, M.; Ehara, M.; Toyota, K.; Fukuda, R.; Hasegawa, J.; Ishida, M.; Nakajima, T.; Honda, Y.; Kitao, O.; Nakai, H.; Klene, M.; Li, X.; Knox, J. E.; Hratchian, H. P.; Cross, J. B.; Bakken, V.; Adamo, C.; Jaramillo, J.; Gomperts, R.; Stratmann, R. E.; Yazyev, O.; Austin, A. J.; Cammi, R.; Pomelli, C.; Ochterski, J. W.; Ayala, P. Y.; Morokuma, K.; Voth, G. A.; Salvador, P.; Dannenberg, J. J.; Zakrzewski, V. G.; Dapprich, S.; Daniels, A. D.; Strain, M. C.; Farkas, O.; Malick, D. K.; Rabuck, A. D.; Raghavachari, K.; Foresman, J. B.; Ortiz, J. V.; Cui, Q.; Baboul, A. G.; Clifford, S.; Cioslowski, J.; Stefanov, B. B.; Liu, G.; Liashenko, A.; Piskorz, P.; Komaromi, I.; Martin, R. L.; Fox, D. J.; Keith, T.; Al-Laham, M. A.; Peng, C. Y.; Nanayakkara, A.; Challacombe, M.; Gill, P. M. W.; Johnson, B.; Chen, W.; Wong, M. W.; Gonzalez, C.; Pople, J. A. *Gaussian 03, Revision D.02*; Gaussian, Inc.: Wallingford, CT, 2004.